Clustered mean-field hard-core model with non-homogeneous clusters

Toshiyuki Tanaka
Graduate School of Informatics
Kyoto University
Kyoto, Japan
Email: tt@i.kyoto-u.ac.jp

Shashi Prabh
School of Engineering and Applied Science
Ahmedabad University
Ahmedabad, India
Email: shashi.prabh@ahduni.edu.in

***Abstract*—This paper addresses modeling and analysis of interference in wireless networks. We present a novel clustered mean-field hard-core model with non-homogeneous clusters. We develop a theory for throughput equalization in this model which can serve as a distributed strategy for throughput equalization. We also present stability analysis of the throughput equalization strategy. This work recovers several previously known results as special cases. We present results of Monte-Carlo simulations to evaluate the proposed strategy in mean-field networks.**

***Index Terms*—Wireless interference, Belief propagation, Mean-field method**

I. Introduction

In this paper, we present a clustered mean-field hard-core model with non-homogeneous clusters, and develop a theory for throughput equalization in this model. This work is motivated by modeling and analysis of interference in wireless networks. Models based on Matérn hard-core point process [1] have been shown to be good models for Carrier Sense Multiple Access with collision avoidance (CSMA/CA) [2], [3]. In networks using time division multiplexing, frequency division multiplexing and CSMA/CA, a node in transmitting state forbids a set of other nodes to be in the same state. We consider a *hard-core model* of interference suited to model this behavior. The model studied in this paper can be interpreted as a special case of the more general loss networks [4], [5]. The belief propagation equations (8) can be regarded as a special form of the Erlang fixed point equations for the loss networks, which are known to give approximate mean activities, and in some limiting regimes asymptotically exact ones.

We studied a collection of interfering nodes in [6]. In this paper, we generalize the model and consider a collection of *clusters* interfering with each other where each cluster consists of m nodes. A "cluster with m nodes" may correspond to a collection of physical devices where each device may use one of m frequency bands. We then assume that if one device uses a frequency band, the other devices in the same cluster cannot use any of the m bands. This "within-cluster interference" is cross-band interference, possibly caused by insufficient attenuation of a signal emitted from a nearby device. The "inter-cluster interference" may be the interference within the same band, that between neighboring bands, or in some other form. In addition to a model for wireless networks of device clusters, "cluster with m nodes" may alternatively correspond to a single physical device that can use any one of the m frequency bands. As this device is allowed to use only one of the m bands, the "within-cluster interference" is such that at most one band is allowed to be active at any given time.

In this paper, we develop a mean field model for interference in a network of clusters of nodes where the inter-cluster interference is modeled by non-geometric conflict graph. In general the cluster degree will vary from cluster to cluster. This leads to lack of fairness in the sense that nodes in clusters with larger degree have the potential of getting hold of the medium for smaller fraction of time as compared to nodes in clusters with smaller degree. This lack of fairness is generally considered harmful since it can cause starvation and bottlenecks. The results of this work serve as a distributed strategy for throughput equalization in the clusters. The conditions under which the throughput equalization remains stable are also presented here. In addition to practical applications, this work recovers several previously known results. As noted above, this work generalizes the results of [6] which was obtained for interference in networks of single nodes where conflict graph edges represented hard-core interaction between a pair of nodes. It should be noted that the mean-field model discussed in [6] was also studied with the different objective of utility maximization in [7]. Constraining the clusters to form a one-dimensional chain, this model includes the linear network with $2m$ nearest-neighbor interactions discussed in [8], [9], [10] as a special case, where it has been analytically shown that throughput equalization can be achieved by appropriately setting the intensity of each node on the basis of its degree. The network with $2 \times L$ rectangular grid topology discussed in [8] can also be regarded as another special case of our framework, by regarding the $2 \times L$ rectangular grid as a one-dimensional chain of L size-2 clusters. The work presented in this paper differs from the above mentioned references in that the cluster of networks model presented in this paper is general and encompasses the other work as special cases. Further, the stability analysis in network of clusters of this paper is new. Stability is not considered in [8], [9], [10]. A study of the application of belief propagation for computing throughput in CSMA networks is presented in [11]. In the above mentioned work, the update messages are set-up and evaluated experimentally. Our present work focuses on throughput equalization and provides closed form expressions. An analysis of average activity in CSMA networks is presented in [12]. This work introduced a mean-field hard-core model of interference and analyzed d-regular graphs. The present work generalizes the model to non-homogeneous clusters.

On the basis of the analogy with the asymptotic exactness of belief propagation decoder of low-density parity-check (LDPC) codes in the limit of infinite codelength [13], belief propagation applied to the mean-field hard-core model gives asymptotically the exact mean activities in the large-system limit. Primarily from the perspective of the relation of the analysis presented here to that of loss networks, the main contributions of this paper are:

1) Derivation of an explicit throughput-equalizing strategy which is local in the sense that the intensity of a node is to be determined only on the basis of the degree of the cluster to which the node belongs and the target mean activity.
2) Proving that there is a threshold in the target mean activity, above which the throughput equalization fails, and that the threshold is given by studying the local stability of belief propagation. The failure of throughput equalization also implies that the Erlang fixed point equations also fail to give good approximations to the mean activities in such cases.

The asymptotic exactness of belief propagation, the efficiency of the proposed throughput-equalizing strategy, as well as the non-trivial correspondence between the failure of the throughput equalization and the local stability of belief propagation are confirmed using numerical experiments.

II. System Model

We consider a collection of clusters of nodes interfering with each other. The within-cluster interference is such that only one node in any cluster can be active simultaneously. The inter-cluster interference is represented by a cluster-level conflict graph, in which clusters are connected by inter-cluster edges, where an inter-cluster edge represents existence of interference between the clusters connected by it. The inter-cluster interference between nodes is expressed as an adjacency matrix of the bipartite conflict graph between nodes in one cluster and those in the other. Given inter-cluster edge CC', the existence/absence of inter-cluster interference between nodes in C and those in C' is represented by a node-level bipartite conflict graph, whose adjacency matrix is denoted by $K_{CC'}$. A node in C and another node in C' cannot be active simultaneously if they have an inter-node edge between them in the node-level conflict graph defined by $K_{CC'}$. The objective is then to adjust the activation rates of nodes in order to achieve equalization, that is, to have the same average activity across all the nodes.

In this paper, we make the following assumptions which allow us to derive an explicit solution achieving equalization exactly for cycle-free graphs, as well as, asymptotically for random graphs in the large-system limit, that is, the limit of the number of clusters tending towards infinity. Let $\{C_a : a = 1, \dots, A\}$ be a partition of C, and $\{C'_a : a = 1, \dots, A'\}$ be a partition of C'. Let $K_{C_a C'_{a'}}$ be the submatrix of $K_{CC'}$ corresponding to the subsets C_a and $C'_{a'}$, that is, $K_{C_a C'_{a'}}$ is the adjacency matrix of the subgraph with the sets of nodes $C_a \cup C'_{a'}$. We assume that all the clusters have the same number m of nodes. Each cluster C admits partitions $\{C_a : a = 1, \dots, A\}$ satisfying the following conditions:

- The number A of the partitions is the same for all the clusters.
- The number of nodes in the A partitions are the same across all the clusters, that is, $|C_a| = s_a$ for any cluster C and any $a \in \{1, \dots, A\}$, whereas $|C_a|$ and $|C_b|$ for $a \neq b$ can be different from each other.
- The subgraph defined by $K_{C_a C'_{a'}}$ is bi-regular. Recall that a bipartite graph $(V \cup V', E)$ is bi-regular if any two nodes in V have the same degree and so do any two nodes in V'. The degree of a node in V and that of a node in V' need not be the same. All the rows of $K_{C_a C'_{a'}}$ have the same sum, and all the columns of $K_{C_a C'_{a'}}$ have the same sum. Furthermore, the row sum $d_{aa'}$ is shared by all the inter-cluster edges.

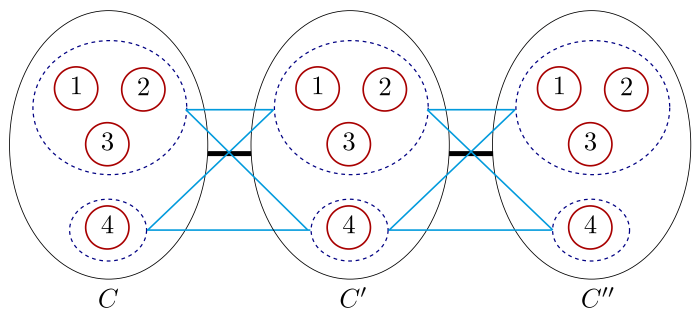

Fig. 1: Conflict graph at cluster level. Partitions are shown in dashed ovals. Interference between different partitions are also shown.

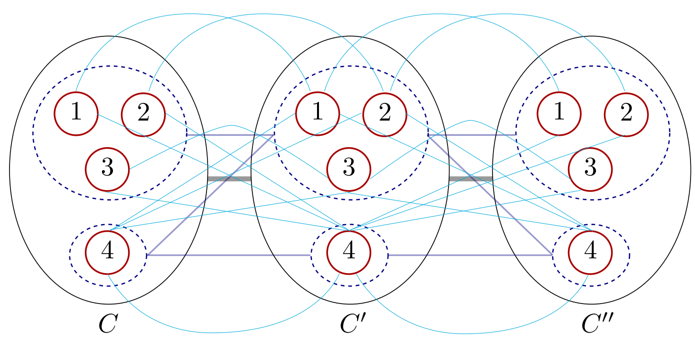

Fig. 2: Conflict graph at node level

An example of clusters satisfying the above conditions is illustrated in Figures 1 and 2. The clusters have two partitions: $C_1 = \{1, 2, 3\}$ and $C_2 = \{4\}$. As $K_{C_a C'_{a'}}$ is of size $s_a \times s_{a'}$ and bi-regular, one has $s_a \geq d_{a'a}$, $s_{a'} \geq d_{aa'}$, and $s_a d_{aa'} =$

$s_{a'}d_{a'a}$ for any a, a'. Let $\boldsymbol{s} = (s_a)$ and $D = (d_{aa'})$. In the above example, one has

$$\boldsymbol{s} = \begin{pmatrix} 3 \\ 1 \end{pmatrix}, \quad D = \begin{pmatrix} 1 & 1 \\ 3 & 1 \end{pmatrix}. \tag{1}$$

Note that a node $i \in C_a$ has degree $\sum_{a'=1}^{A} d_{aa'} = (D\mathbf{1})_a$.

III. Belief Propagation

Let $\boldsymbol{\Psi}_C \in \{\mathbf{0}, \boldsymbol{e}_1, \ldots, \boldsymbol{e}_m\}$ denote the state of cluster C, where $\{\boldsymbol{e}_1, \ldots, \boldsymbol{e}_m\}$ is the standard basis of an m-dimensional space, with $\boldsymbol{e}_i$ representing the state that node i in the cluster is active while the remaining $(m-1)$ nodes are inactive. Similarly, let $\boldsymbol{\Psi}_{C_a} \in \{\mathbf{0}, \boldsymbol{e}'_1, \ldots, \boldsymbol{e}'_{s_a}\}$ denote the state of a partition, where $\boldsymbol{e}'_i$ is an s_a-dimension vector whose i^{th} element is 1 and all other elements are 0. The mean activity of a partition C_a is

$$\rho_{C_a} = \sum_{\boldsymbol{\Psi}_{C_a} \neq \mathbf{0}} P(\boldsymbol{\Psi}_{C_a}; \mu_{C,a}), \tag{2}$$

where P is the probability distribution of the state vector and $\mu_{C,a}$ is the activation rate controlling the average activity of nodes in partition C_a. The parameter μ is analogous to the chemical potential used in statistical mechanics.

We use the factor graph representation [14] of the conflict graph to apply belief propagation [15]. A factor graph is a bipartite graph containing $|V|$ variable nodes, each corresponding to a cluster partition, and $|E|$ factor nodes, each corresponding to a hard-core constraint. An edge in the factor graph connects a variable node and a factor node representing a hard-core constraint on the variable node. More concretely, we model the joint distribution of the cluster states $\boldsymbol{\Psi} = (\boldsymbol{\Psi}_C)$ as

$$P(\boldsymbol{\Psi}; \boldsymbol{\mu}) \propto \prod_{C \in V} P_0(\boldsymbol{\Psi}_C; \boldsymbol{\mu}_C) \prod_{CC' \in E} \Phi(\boldsymbol{\Psi}_C, \boldsymbol{\Psi}_{C'}; K_{CC'}), \tag{3}$$

where

$$P_0(\boldsymbol{\Psi}_C; \boldsymbol{\mu}_C) \propto e^{\sum_{i=1}^{m} \delta_{\boldsymbol{\Psi}_C, \boldsymbol{e}_i} \mu_{C,i}}, \tag{4}$$

Kronecker's delta $\delta_{\cdot,\cdot}$, governs the probabilistic activity of cluster C *if there were no inter-cluster interference*, and

$$\Phi(\boldsymbol{\Psi}_C, \boldsymbol{\Psi}_{C'}; K_{CC'}) = 1 - \boldsymbol{\Psi}_C^\top K_{CC'} \boldsymbol{\Psi}_{C'} \tag{5}$$

represents the inter-cluster interference between clusters C and C'. The factor model we consider consists of variable nodes, each of which corresponds to the state variable $\boldsymbol{\Psi}_C$ of a cluster, and factor nodes, each of which corresponds to an inter-cluster constraint.

Our goals are to evaluate the mean activities $\{\rho_{C_a}\}$ given the activation rates $\boldsymbol{\mu}$ under the probability model (3), and furthermore, to determine $\boldsymbol{\mu}$ to achieve equalization. Our starting point is the observation that belief propagation is applicable to deal with the former problem, in which one considers, for each edge C_a–$(C_aC'_{a'})$ connecting variable node $C_a \in V$ and factor node $(C_aC'_{a'}) \in E$ in the factor graph, two messages $\pi_{C_a \to (C_aC'_{a'})}$ and $\pi_{(C_aC'_{a'}) \to C_a}$, the former being from variable node C_a to factor node $(C_aC'_{a'})$, and the other from factor node $(C_aC'_{a'})$ to variable node C_a. Each node collects messages from adjacent nodes in the factor graph, and calculates messages to be sent to the adjacent nodes. Since each factor node is of degree 2, which reflects the fact that each hard-core constraint is on two variables, the message $\pi_{(C_aC'_{a'}) \to C_a}$ from factor node $(C_aC'_{a'})$ to variable node C_a is the same as the message $\pi_{C'_{a'} \to (C_aC'_{a'})}$ to the factor node $(C_aC'_{a'})$ from the other variable node $C'_{a'}$ connected to the factor node. One can then define the message $\pi_{C_a \to C'_{a'}}$ for edge $(C_aC'_{a'})$ in the conflict graph as being equal to $\pi_{C_a \to (C_aC'_{a'})}$ and $\pi_{(C_aC'_{a'}) \to C'_{a'}}$. Since the messages $\pi_{C_a \to C'_{a'}}$ can be regarded as probability distributions of $\boldsymbol{\Psi}_{C_a}$, the state vector of partition C_a, these messages are simply parameterized by their respective expectations. With a slight abuse of notation, we let $\boldsymbol{\pi}_{C_a \to C'_{a'}} \in [0,1]^{s_a}$ denote the expectation of the message from node C_a to node $C'_{a'}$ in G, and call such parameters the messages.

Consider clusters C and C' that are connected by an inter-cluster edge in the conflict graph. Let $(C_aC'_{a'})$ denote the factor node representing the interaction between the partitions C_a and $C'_{a'}$. Application of belief propagation to throughput equalization in the hard-core model gives the message update formula (3), where $\mu_{C,a,i}$ is the intensity of device $i \in C_a$ and $\partial C_a \backslash C'_{a'}$ denotes the set of neighbors of C_a excluding $C'_{a'}$.

The mean activity of device $i \in C_a$ is evaluated using converged messages as

$$\rho_i = \frac{e^{\mu_{C,a,i}} \prod_{C'_{a'} \in \partial C_a} \left(1 - (K_{C_aC'_{a'}} \boldsymbol{\pi}_{C'_{a'} \to C_a})_i\right)}{1 + \sum_{j=1}^{A} \sum_{i'=1}^{s_j} e^{\mu_{C,j,i'}} \prod_{C'_{a'} \in \partial C_j} \left(1 - (K_{C_jC'_{a'}} \boldsymbol{\pi}_{C'_{a'} \to C_j})_{i'}\right)}. \tag{7}$$

IV. Throughput Equalization

Suppose that there exists an equilibrium message $\bar{\boldsymbol{\pi}} = (\bar{\pi}_a)$, meaning that the outgoing message from node $i \in C_a$ at equilibrium is $\bar{\pi}_a$ for each cluster C. For C, C' and $i \in C_a$, one has $(K_{CC'}\bar{\boldsymbol{\pi}})_i = \sum_{a'=1}^{A} d_{aa'} \bar{\boldsymbol{\pi}}_{a'} = (D\bar{\boldsymbol{\pi}})_a$, and the belief propagation equation at equilibrium reads

$$\bar{\pi}_a = \frac{e^{\mu_{C,a}} (1 - (D\bar{\boldsymbol{\pi}})_a)^{|\partial C| - 1}}{1 + \sum_{a'=1}^{A} s_{a'} e^{\mu_{C,a'}} (1 - (D\bar{\boldsymbol{\pi}})_{a'})^{|\partial C| - 1}}. \tag{8}$$

Using the equilibrium messages $\bar{\boldsymbol{\pi}}$, the mean activity ρ_a of nodes in C_a is given by

$$\rho_a = \frac{e^{\mu_{C,a}} (1 - (D\bar{\boldsymbol{\pi}})_a)^{|\partial C|}}{1 + \sum_{a'=1}^{A} s_{a'} e^{\mu_{C,a'}} (1 - (D\bar{\boldsymbol{\pi}})_{a'})^{|\partial C|}}. \tag{9}$$

Although the above expression for the mean activities may not be correct if the graph has cycles, it becomes exact asymptotically for random conflict graphs in the large-system limit. In the following, we assume either a cycle-free graph or the large-system limit of such random conflict graphs.

The expression (8) shows that if one can choose $\mu_{C,a}$ depending on the degree of C so that $e^{\mu_{C,a}}(1 - (D\bar{\boldsymbol{\pi}})_a)^{|\partial C| - 1}$ becomes independent of C, then $\bar{\boldsymbol{\pi}}$ becomes an equilibrium

$$\pi_{C_a\to C'_{a'},i} = \frac{e^{\mu_{C,a,i}}\prod_{C''_{a''}\in\partial C_a\setminus C'_{a'}}\left(1-(K_{C_aC''_{a''}}\boldsymbol{\pi}_{C''_{a''}\to C_a})_i\right)}{1+\sum_{j=1}^{A}\sum_{i'=1}^{s_j}e^{\mu_{C,j,i'}}\prod_{C''_{a''}\in\partial C_j\setminus C'_{a'}}\left(1-(K_{C_aC''_{a''}}\boldsymbol{\pi}_{C''_{a''}\to C_a})_{i'}\right)},\quad i=1,\dots,s_a \tag{3}$$

---

message vector, that is, the outgoing message vector of a cluster is $\bar{\boldsymbol{\pi}}$ when all the incoming message vectors to the cluster are $\bar{\boldsymbol{\pi}}$, and this holds for every cluster. In other words, the inter-cluster equalization is achieved asymptotically.

Assuming that one chooses such $\mu_{C,a}$'s, and letting $\boldsymbol{p}=(p_a)$ with $p_a=e^{\mu_{C,a}}(1-(D\bar{\boldsymbol{\pi}})_a)^{|\partial C|-1}$, one has

$$\bar{\pi}_a=\frac{p_a}{1+\sum_{a'=1}^{A}s_{a'}p_{a'}}=\frac{p_a}{1+\boldsymbol{s}^T\boldsymbol{p}}, \tag{10}$$

which is summarized in a vector form as

$$\bar{\boldsymbol{\pi}}=\frac{\boldsymbol{p}}{1+\boldsymbol{s}^T\boldsymbol{p}}. \tag{11}$$

We can solve it with respect to $\boldsymbol{p}$ as

$$\bar{\boldsymbol{\pi}}=(I-\bar{\boldsymbol{\pi}}\boldsymbol{s}^T)\boldsymbol{p}, \tag{12}$$

$$\begin{aligned}\boldsymbol{p}&=(I-\bar{\boldsymbol{\pi}}\boldsymbol{s}^T)^{-1}\bar{\boldsymbol{\pi}}\\&=\left(I+\frac{\bar{\boldsymbol{\pi}}\boldsymbol{s}^T}{1-\boldsymbol{s}^T\bar{\boldsymbol{\pi}}}\right)\bar{\boldsymbol{\pi}}\\&=\left(1+\frac{\boldsymbol{s}^T\bar{\boldsymbol{\pi}}}{1-\boldsymbol{s}^T\bar{\boldsymbol{\pi}}}\right)\bar{\boldsymbol{\pi}}\\&=\frac{\bar{\boldsymbol{\pi}}}{1-\boldsymbol{s}^T\bar{\boldsymbol{\pi}}},\end{aligned} \tag{13}$$

where we have used the identity

$$(I-\boldsymbol{a}\boldsymbol{b}^T)^{-1}=\left(I+\frac{\boldsymbol{a}\boldsymbol{b}^T}{1-\boldsymbol{b}^T\boldsymbol{a}}\right). \tag{14}$$

Letting $q_a=(1-(D\bar{\boldsymbol{\pi}})_a)p_a$, one has

$$\begin{aligned}\rho_a&=\frac{(1-(D\bar{\boldsymbol{\pi}})_a)p_a}{1+\sum_{a'=1}^{A}s_{a'}p_{a'}(1-(D\bar{\boldsymbol{\pi}})_{a'})}\\&=\frac{q_a}{1+\sum_{a'=1}^{A}s_{a'}q_{a'}}.\end{aligned} \tag{15}$$

Within-cluster equalization will be achieved if one can let q_a be independent of a, which in turn makes ρ_a independent of a. As we have already achieved inter-cluster equalization, letting q_a be independent of a allows us to achieve perfect equalization. Assume $q_a=q$. One then has

$$\begin{aligned}q\mathbf{1}&=(I-\mathrm{diag}(D\bar{\boldsymbol{\pi}}))\boldsymbol{p}\\&=\left(I-\frac{1}{1+\boldsymbol{s}^T\boldsymbol{p}}\mathrm{diag}(D\boldsymbol{p})\right)\boldsymbol{p},\\q(1+\boldsymbol{s}^T\boldsymbol{p})\mathbf{1}&=\left((1+\boldsymbol{s}^T\boldsymbol{p})I-\mathrm{diag}(D\boldsymbol{p})\right)\boldsymbol{p}\end{aligned} \tag{16}$$

The tunable parameters are $\{\mu_{C,a}\}$. If one can find $\boldsymbol{p}$ satisfying the above condition, then one can calculate $\bar{\boldsymbol{\pi}}$ via (11), and finally one may be able to specify $\mu_{C,a}$ via $p_a=e^{\mu_a}(1-(D\bar{\boldsymbol{\pi}})_a)^{|\partial C|-1}$ according to $\bar{\boldsymbol{\pi}}$ and the degree $|\partial C|$ of the cluster C. This establishes the following theorem:

Theorem 1 (Throughput equalization in inhomogeneous clusters): In a network of inhomogeneous clusters, the per-node throughput in a cluster C is equalized if the intensity $\mu_{C,a}$ of nodes in its partitions $a\in\{1,\dots,A\}$ are chosen according to $p_a=e^{\mu_{C,a}}(1-(D\bar{\boldsymbol{\pi}})_a)^{|\partial C|-1}$ where $\boldsymbol{p}=(p_a)$ satisfies (16) for a given equalization target q.

The iteration

$$p_a^{(t+1)}:=\frac{q}{1-\frac{(D\boldsymbol{p}^{(t)})_a}{1+\boldsymbol{s}^T\boldsymbol{p}^{(t)}}} \tag{17}$$

starting from the initialization $\boldsymbol{p}^{(0)}=\mathbf{0}$ can be used for numerically finding the solution $\boldsymbol{p}$ for a given value of q.

Convergence proof of (17)*:* Simplifying (17) gives

$$p_a^{(t+1)}:=\frac{q(1+\boldsymbol{s}^T\boldsymbol{p}^{(t)})}{1+\sum_{a'=1}^{A}(s_{a'}-d_{aa'})p_{a'}^{(t)}}. \tag{18}$$

Since $s_{a'}\ge d_{aa'}$ for all a,a', and $p_a^{(t)}\ge 0$,

$$p_a^{(t+1)}\le q(1+\boldsymbol{s}^T\boldsymbol{p}^{(t)}). \tag{19}$$

Let $\alpha=\mathrm{argmax}_a\sum_{a'=1}^{A}d_{aa'}$ and define

$$\tilde{p}_\alpha^{(t+1)}:=q(1+m\tilde{p}_\alpha^{(t)}), \tag{20}$$

where $\tilde{p}_\alpha^{(0)}=0$. Clearly, $\tilde{p}_\alpha^{(t+1)}\ge p_a^{(t+1)}$, $\forall t\ge 0$ and for all $a=1,\dots,A$. We now show that $\tilde{p}_\alpha^{(t)}$ converges if $qm<1$, thereby establishing the iteration (17) being non-diverging. The iteration (20) is solved as

$$\tilde{p}_\alpha^{(t)}=q\frac{1-(qm)^t}{1-qm}, \tag{21}$$

which converges if $qm<1$. ■

Special cases (homogeneous clusters): Assume that $D\mathbf{1}=k\mathbf{1}$, that is, row sums of $K_{CC'}$ are all equal to k. We seek an equalized solution under this assumption. Suppose $\bar{\boldsymbol{\pi}}=\bar{\pi}\mathbf{1}$ and $\boldsymbol{p}=p\mathbf{1}$. Then one has $D\bar{\boldsymbol{\pi}}=k\bar{\pi}\mathbf{1}$, $\bar{\pi}=\frac{p}{1+mp}$, and $p=\frac{\bar{\pi}}{1-m\bar{\pi}}$. Choosing μ_a to satisfy

$$\mu_a=\log\frac{p}{(1-k\bar{\pi})^{|\partial C|-1}}=\log\frac{\bar{\pi}}{(1-m\bar{\pi})(1-k\bar{\pi})^{|\partial C|-1}} \tag{22}$$

one has

$$\rho=\frac{q}{1+mq} \tag{23}$$

with $q=(1-k\bar{\pi})p=\frac{\bar{\pi}(1-k\bar{\pi})}{1-m\bar{\pi}}$, achieving throughput equalization. This implies

$$\begin{aligned}\rho&=\frac{q}{1+mq}=\frac{\frac{\bar{\pi}(1-k\bar{\pi})}{1-m\bar{\pi}}}{1+m\frac{\bar{\pi}(1-k\bar{\pi})}{1-m\bar{\pi}}}\\&=\frac{\bar{\pi}(1-k\bar{\pi})}{1-m\bar{\pi}+m\bar{\pi}(1-k\bar{\pi})}=\frac{\bar{\pi}(1-k\bar{\pi})}{1-mk\bar{\pi}^2},\end{aligned} \tag{24}$$

reproducing the result of [16].

By letting $k = m = 1$, the above equations recover the results of [6].

Further, constraining the clusters to form a one-dimensional chain, the homogeneous cluster case includes the linear network with $2m$ nearest-neighbor interactions discussed in [8], [9], [10] as a special case. Their result can be reproduced within this paper's framework since a one-dimensional chain with $2m$ nearest-neighbor interaction can be regarded as a one-dimensional chain of size-m clusters, which is cycle-free. Belief propagation used in our work becomes exact when it is applied to trees, which includes one-dimensional chain as a special case. Specializing the above result to the case of a length-L linear network of clusters with $m = 2$ and $k = 1$ reproduces the result in [8] on the rectangular grid of size $2 \times L$.

It should be noted that our model also includes as a special case the multi-channel linear networks [17] with 2 nearest-neighbor interactions, by letting $K_{CC'} = I$ for all C, C' connected by an inter-cluster edge, which yields $k = 1$. Although the authors of [17] mentioned that no simple formula achieving equalization would seem to exist except under heavy traffic, our result successfully demonstrates that such a formula does exist in some cases.

V. Local stability analysis

We study local stability of the equalizing solution $\bar{\boldsymbol{\pi}}$ via considering small perturbations of the messages around the equalizing solution.

Theorem 2 (Stability of throughput equalization): The throughput equalization strategy given by Theorem 1 is stable if $\left(\frac{\xi_{\mathcal{B}}\nu_{\mathcal{K}}}{q(1+\boldsymbol{s}^T\boldsymbol{p})}\right)^2 < 1$ where $\xi_{\mathcal{B}}$ is the largest eigenvalue of the nonbacktracking matrix, $\mathcal{B}$, of the conflict graph and $\nu_{\mathcal{K}}$ is the largest eigenvalue of $\mathcal{K}$ given by (31).

Proof: We first consider how a perturbation of an incoming message to a cluster affects an outgoing message from the cluster. We specifically assume that all the incoming messages to cluster C are the equalizing message $\bar{\boldsymbol{\pi}}$ except the one from cluster C' that is adjacent to C, which is assumed to have element j perturbed as

$$\boldsymbol{\pi}_{C' \to (C'C)} = \bar{\boldsymbol{\pi}} + \delta_{C'C,j}\boldsymbol{e}_j. \tag{25}$$

This perturbation of the incoming message from cluster C' causes perturbation of the outgoing message to cluster $B \neq C'$ as

$$\begin{aligned}
&\delta_{CB,i} = \\
&\left[-(K_{CC'})_{ij}\frac{e^{\mu_{C,i}}\prod_{D'\in\partial C\backslash B,C'}(1-(K_{CD'}\bar{\boldsymbol{\pi}})_i)}{1+\sum_{i'=1}^{m_C}e^{\mu_{C,i'}}\prod_{D'\in\partial C\backslash B}(1-(K_{CD'}\bar{\boldsymbol{\pi}})_{i'})}\right.\\
&\left.+\bar{\pi}_i\frac{\sum_{i'=1}^{m_C}e^{\mu_{C,i'}}(K_{CC'})_{i'j}\prod_{D'\in\partial C\backslash B,C'}(1-(K_{CD'}\bar{\boldsymbol{\pi}})_{i'})}{1+\sum_{i'=1}^{m_C}e^{\mu_{C,i'}}\prod_{D'\in\partial C\backslash B}(1-(K_{CD'}\bar{\boldsymbol{\pi}})_{i'})}\right]\\
&\times\delta_{C'C,j}.
\end{aligned} \tag{26}$$

It should be noted that when $i \in C_a$ one has $K_{CD'}\bar{\boldsymbol{\pi}} = D\bar{\boldsymbol{\pi}}$, which is independent of D'. Also note that when $j \in C'_b$, $\sum_{i'\in C_a}(K_{CC'})_{i'j}$ is equal to the column sum of $K_{C_aC'_b}$, which is further equal to the row sum of $K_{C'_bC_a}$, which is d_{ba}. Using these, the above expression is reduced to

$$\begin{aligned}
&\delta_{CB,i} = \\
&\quad\left[-(K_{CC'})_{ij}\frac{e^{\mu_{C,a}}(1-(D\bar{\boldsymbol{\pi}})_a)^{|\partial C|-2}}{1+\sum_{a'=1}^{A}s_{a'}e^{\mu_{C,a'}}(1-(D\bar{\boldsymbol{\pi}})_{a'})^{|\partial C|-1}}\right.\\
&\quad\left.+\bar{\pi}_a\frac{\sum_{a'=1}^{A}e^{\mu_{C,a'}}d_{ba'}(1-(D\bar{\boldsymbol{\pi}})_{a'})^{|\partial C|-2}}{1+\sum_{a'=1}^{A}s_{a'}e^{\mu_{C,a'}}(1-(D\bar{\boldsymbol{\pi}})_{a'})^{|\partial C|-1}}\right]\delta_{C'C,j}\\
&\quad=\left[-(K_{CC'})_{ij}\frac{r_a}{1+\boldsymbol{s}^T\boldsymbol{p}}+\bar{\pi}_a\frac{\sum_{a'=1}^{A}d_{ba'}r_{a'}}{1+\boldsymbol{s}^T\boldsymbol{p}}\right]\delta_{C'C,j},
\end{aligned} \tag{27}$$

where we have let

$$\begin{aligned}
r_a &= e^{\mu_{c,a}}(1-(D\bar{\boldsymbol{\pi}})_a)^{|\partial C|-2} = \frac{p_a}{1-(D\bar{\boldsymbol{\pi}})_a}\\
&= \frac{q}{(1-(D\bar{\boldsymbol{\pi}})_a)^2} = \frac{p_a^2}{q}.
\end{aligned} \tag{28}$$

Let $\boldsymbol{z} = (z_a)$ with $z_a = p_a^2$. One then has

$$\delta_{CB,i} = \frac{1}{q(1+\boldsymbol{s}^T\boldsymbol{p})}\left[\bar{\pi}_a(D^T\boldsymbol{z})_b - (K_{CC'})_{ij}z_a\right]\delta_{C'C,j}. \tag{29}$$

The coefficient of $\delta_{C'C,j}$ on the right-hand side gives the corresponding element of the Jacobian $\mathcal{J}$ associated with the message-updating formulas at the equalizing solution.

If we further assume that $K_{CC'} = K$ for every edge CC' in the graph, then the Jacobian $\mathcal{J}$ is represented as

$$\mathcal{J} = \frac{1}{q(1+\boldsymbol{s}^T\boldsymbol{p})}\mathcal{B}\otimes\mathcal{K}, \tag{30}$$

where $\mathcal{B}$ is what is called the nonbacktracking matrix of the graph [18] and

$$\mathcal{K} = (k_{ij}), \quad k_{ij} = \bar{\pi}_a(D^T\boldsymbol{z})_b - K_{ij}z_a, \quad i \in C_a, j \in C_b. \tag{31}$$

Let $\nu_{\mathcal{K}}$ and $\xi_{\mathcal{B}}$ be the maximal eigenvalues of $\mathcal{K}$ and $\mathcal{B}$, respectively. Then the stability condition is given by [18]:

$$\left(\frac{\xi_{\mathcal{B}}\nu_{\mathcal{K}}}{q(1+\boldsymbol{s}^T\boldsymbol{p})}\right)^2 < 1. \tag{32}$$

■

We may instead assume that $K_{CC'}$ are chosen randomly among those satisfying the degree constraints specified by the matrix D, in which case the local stability analysis would be much more complicated than that in the case with $K_{CC'} = K$. The local stability condition should depend on the details of the assumptions on $K_{CC'}$.

Special case: Assume that $K = \mathbf{1}\mathbf{1}^T$, that is, K is the complete bipartite graph, and that the graph is a sample from a random ensemble of large sparse graphs specified by a degree distribution $\lambda(d)$. One then has

$$\xi_{\mathcal{B}} = \sqrt{c}, \tag{33}$$

where

$$c = \frac{\sum_d d^2\lambda(d)}{\sum_d d\lambda(d)} - 1. \tag{34}$$

One also has

$$\bar{\pi} = \frac{p}{1+mp}, \quad p = \frac{\bar{\pi}}{1-m\bar{\pi}}, \quad q = (1-m\bar{\pi})p = \bar{\pi},$$
$$q(1+\boldsymbol{s}^T\boldsymbol{p}) = \bar{\pi}(1+mp) = p, \tag{35}$$

so that $\mathcal{K}$ is given by

$$\mathcal{K} = (m\bar{\pi}-1)p^2\mathbf{1}\mathbf{1}^T = -\bar{\pi}p\mathbf{1}\mathbf{1}^T, \tag{36}$$

yielding $\nu_{\mathcal{K}} = -m\bar{\pi}p$. Collecting these results, the stability condition for this special case reduces to $cm^2\bar{\pi}^2 < 1$, which reproduces the stability condition given as equation (17) in [16].

VI. Numerical results

A. Non-homogeneous clusters

We now present numerical results that evaluate the performance of the throughput equalization method. The interference scenario in the simulations are based on the examples discussed in Section II. Node i in a cluster interferes with node i in adjacent clusters and also nodes $i-1$ and $i+1$ in those clusters whenever such nodes exist. Clusters are connected by an edge with probability p. Further, clusters are ensured to be connected. The partition sizes are kept 2 if the number of nodes in clusters is even. Otherwise, the sizes of all but one partition is kept 2 and one of the partitions consists of one node. We present data for the odd m case below. The results for even m were similar and hence omitted. We simulated two scenarios where network consisted of 10 and 30 clusters, respectively.

Using q as the independent variable, we first calculated $\bar{\boldsymbol{\pi}}$ using (11) and then $\mu_{C,a}$ was obtained as $p_a = e^{\mu_a}(1-(D\bar{\boldsymbol{\pi}})_a)^{|\partial C|-1}$. We randomly selected a node and performed Monte-Carlo updates of its state taking into account the hard-core interactions. After a burn-in period we computed the activities of the nodes in the network. The total Monte-Carlo steps for each q were set to 10^6.

Figures 3 and 4 show the performance of throughput equalization for networks where average cluster degrees were 3.6 and 8.1 for the network of 10 clusters and 3.9 and 9.9 for the network of 30 clusters, respectively. Each of the two cases represent networks with 10 and 30 clusters where each cluster had four partitions of sizes 2, 2, 2 and 1. In addition to the average node activity for all the nodes, the figures also show the average node activity in three randomly chosen clusters. The range of values of q for which the stability condition (32) is satisfied is shown by a horizontal line on the bottom of each of the plots.

Average *node activity* is shown on the vertical axis. Since each cluster has 7 nodes, the maximum average cluster activity achieved within the stability region for Figure 3 is between 0.4 and 0.5. Some non-negligible variance in average activity within the stability region was due to small system size and low cluster degree. In networks with larger cluster degrees, there was very good agreement between theory and simulation results as shown in Figure 4. We see that the variance starts to rise beyond the stability region.

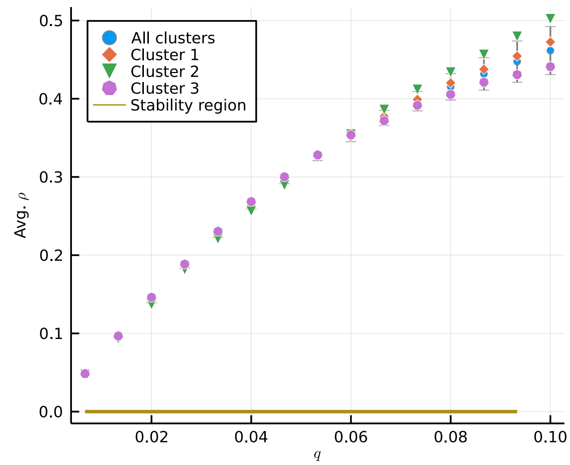

(a) 10 clusters.

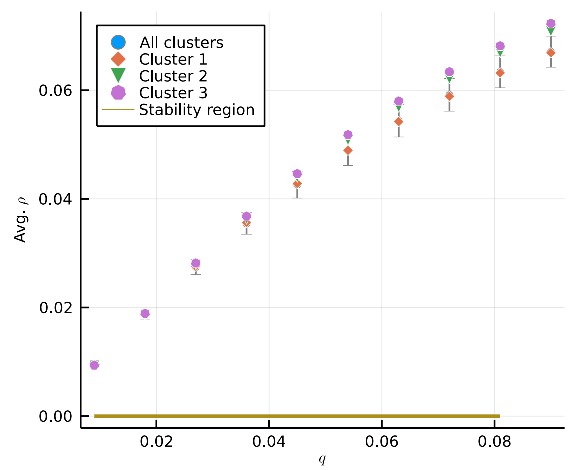

(b) 30 clusters.

Fig. 3: Average cluster degree ≈ 4.

B. Homogeneous clusters

The closed-form expressions for homogeneous clusters allow simulations and evaluation of the theoretical results on large networks. Here we simulated networks of 1000 clusters. We first generated inter-cluster conflict graph. We used the approach taken in [6] to compute a graphical degree sequence of prescribed degree distribution. Subsequently, we used the algorithms of [19], [20] to generate graphs that conform to the graphical degree sequence obtained earlier. Then we connected each node in one cluster to k nodes in each of the adjacent clusters in the conflict graph. We do so systematically by connecting a node, i, to nodes i, …, $(i+k-1)\%m$.

We performed Monte-Carlo updates of the states of the clusters as in the simulations of non-homogeneous clusters. In a typical Monte-Carlo step, if a cluster has none of its nodes active, it is decided to be turned on with probability

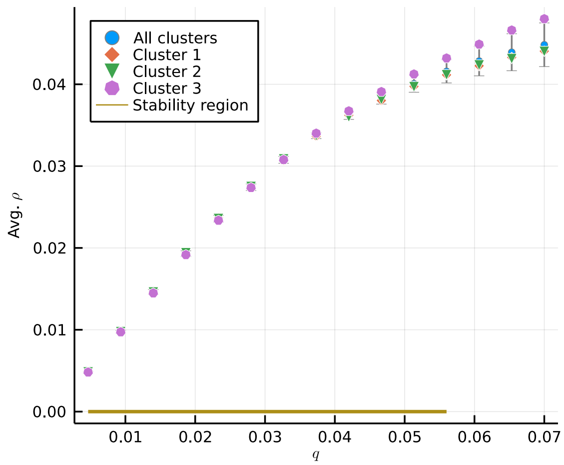

(a) 10 clusters.

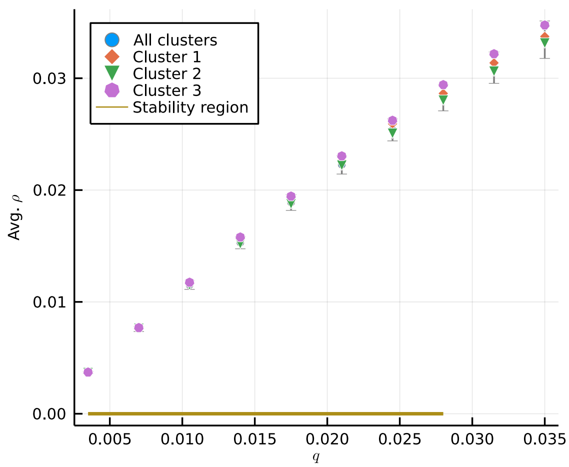

(b) 30 clusters.

Fig. 4: Average cluster degree ≈ 9.

$e^{\mu_a}/(1+e^{\mu_a})$ (22). If a cluster is decided to be turned on, we search for a non-blocked node in the cluster and turn it on. If several nodes can be turned on, we make a list of all such nodes and randomly select one node among the list to be turned on. Note that it is possible for two clusters connected by a conflict edge to be simultaneously active (Fig. 5).

Results of simulation of $m = 6$ cluster models with varying k are shown in Figs. 6a–6b. The cluster degree distribution is uniform over the degrees from 3 to 6. Each figure represents a network of 1000 clusters and each data point represents a result obtained from about 10^9 MC steps. The target node activity $\bar{\rho}$ is the independent variable and the average cluster activity is shown on the Y-axis. The dashed line represent ideal equalized node throughput. Similarly to the case of non-homogeneous clusters, the range of the target $\bar{\rho}$ values over

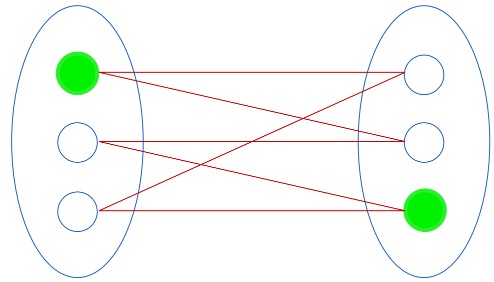

Fig. 5: Two neighboring clusters can be simultaneously active as shown in this model with $m = 3, k = 2$.

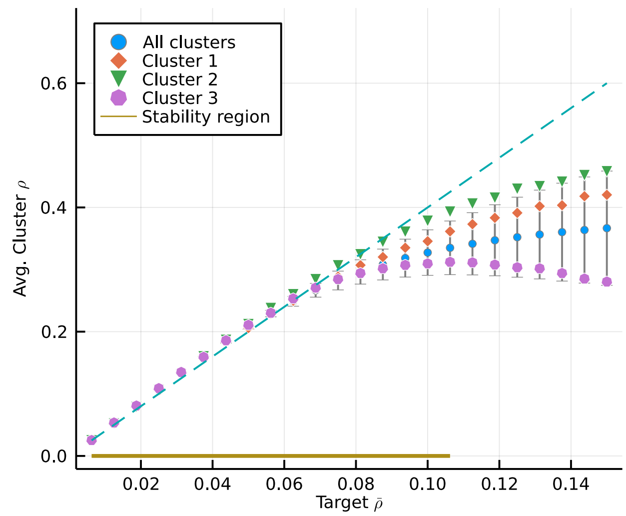

(a) $m = 4, k = 2$.

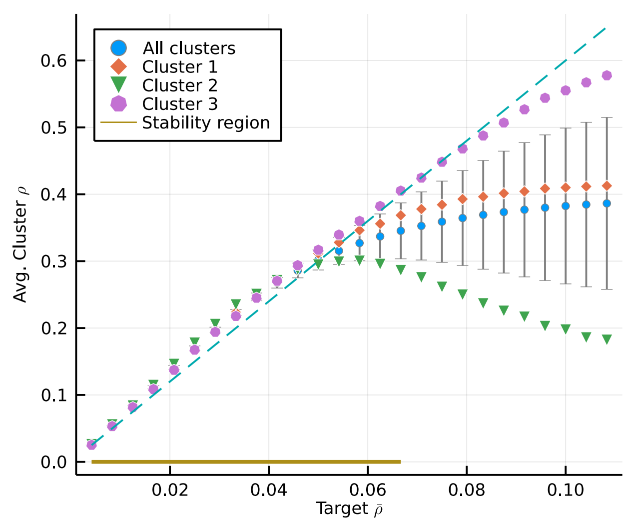

(b) $m = 6, k = 4$.

Fig. 6: Throughput equalization performance. 1000 clusters.

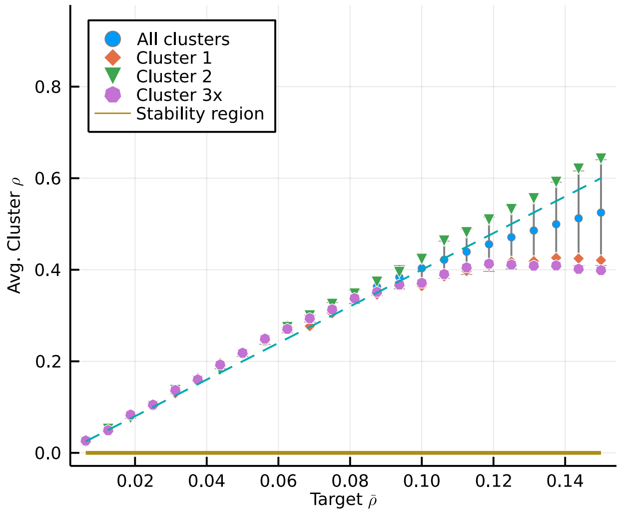

Fig. 7: Throughput equalization in a tree. $m = 4, k = 2$.

which the equalization strategy is predicted to be stable is shown by the horizontal line. We observe that the equalization strategy is effective even though the simulated graphs had cycles. As the target $\bar{\rho}$ approaches the stability threshold, the clusters whose inter-cluster degree is larger than the average start to get lower throughput than the average. "Cluster 3" in Fig. 6a and "Cluster 2" in Fig. 6b are such examples.

Figure 7 shows the simulation result where the cluster conflict graph was a tree. There were 1000 clusters where we first generated the conflict graph as described above and then removed edges from loops until the graph was a tree. The result was that 422 clusters had degree 1, 289 had degree 2, 186 had degree 3, 73 had degree 4 and 30 had degree 5.

VII. Conclusion

In this paper we introduced a clustered mean-field hard-core model for non-homogeneous clusters. We developed a theory for throughput equalization and stability analysis. Based on this theory, we obtained local methods to equalize throughput and derived conditions for its stability. The work presented here is a generalization of previously reported results in the literature. The results for homogeneous clusters were shown to be a special case. We presented results of Monte-Carlo simulations for non-homogeneous and homogeneous clusters that confirm the effectiveness of the proposed strategy as well as the presence of instability.

Acknowledgment

Toshiyuki Tanaka acknowledges support of MEXT KAKENHI Grant Numbers JP25120008 and JP18079010. Shashi Prabh acknowledges support of the Ahmedabad University grant number URBSEASE20A6/SUG/20-21/03-SP-08.23.

References

[1] B. Matérn, *Spatial Variation*, 2nd ed., ser. Springer Lecture Notes in Statistics, 1986, vol. 36.

[2] M. Haenggi, "Mean interference in hard-core wireless networks," *IEEE Communications Letters*, vol. 15, no. 8, pp. 792–794, Aug. 2011.

[3] U. Schilcher, J. F. Schmidt, and C. Bettstetter, "On interference dynamics in Matérn networks," *IEEE Transactions on Mobile Computing*, vol. 19, no. 7, pp. 1677–1688, 2020.

[4] F. P. Kelly, "Loss networks," *Annals of Applied Probability*, vol. 1, no. 3, pp. 319–378, August 1991.

[5] F. Kelly and E. Yudovina, *Stochastic Networks*. Cambridge University Press, 2014.

[6] T. Tanaka, K. S. Prabh, and Y. Liu, "Throughput equalization in mean-field hard-core models for CSMA-based wireless networks," in *Proc. 14th International Symposium on Modeling and Optimization in Mobile, Ad Hoc, and Wireless Networks (WiOpt)*, May 2016, pp. 329–336.

[7] S.-Y. Yun, J. Shin, and Y. Yi, "CSMA using the Bethe approximation: Scheduling and utility maximization," *IEEE Transactions on Information Theory*, vol. 61, no. 9, pp. 4776–4787, Sep. 2015.

[8] P. M. van de Ven, S. C. Borst, D. Denteneer, A. J. E. M. Janssen, and J. S. H. van Leeuwaarden, "Equalizing throughputs in random-acceess networks," *ACM SIGMETRICS Performance Evaluation Review*, vol. 38, no. 2, pp. 39–41, Sept. 2010.

[9] P. M. van de Ven, A. J. E. M. Janssen, J. S. H. van Leeuwaarden, and S. C. Borst, "Achieving target throughputs in random-access networks," *Performance Evaluation*, vol. 68, no. 11, pp. 1103–1117, Nov. 2011.

[10] P. M. van de Ven, J. S. H. van Leeuwaarden, D. Denteneer, and A. J. E. M. Janssen, "Spatial fairness in linear random-access networks," *Performance Evaluation*, vol. 69, no. 3-4, pp. 121–134, Mar.–Apr. 2012.

[11] C. H. Kai and S. C. Liew, "Applications of belief propagation in CSMA wireless networks," *IEEE/ACM Transactions on Networking*, vol. 20, no. 4, pp. 1276–1289, 2012.

[12] T. Tanaka and K. S. Prabh, "Mean-field hard-core model of interference in ad-hoc wireless networks," in *Proc. 53rd Annual Allerton Conference on Communication, Control, and Computing (Allerton)*, Sept 2015, pp. 279–285.

[13] T. Richardson and R. Urbanke, *Modern Coding Theory*. Cambridge University Press, 2008.

[14] F. Kschischang, B. Frey, and H.-A. Loeliger, "Factor graphs and the sum-product algorithm," *IEEE Transactions on Information Theory*, vol. 47, no. 2, pp. 498–519, 2001.

[15] J. S. Yedidia, W. T. Freeman, and Y. Weiss, "Understanding belief propagation and its generalizations," in *Exploring artificial intelligence in the new millennium*, 2003, pp. 239–269.

[16] Y. Liu, T. Tanaka, and K. S. Prabh, "Throughput equalization for CSMA-based wireless networks using mean-field hard-core model," Technical Report of IEICE, Tech. Rep. 115(484), 2016.

[17] R. Block and B. V. Houdt, "Spacial fairness in multi-channel CSMA line networks," *Performance Evaluation*, vol. 103, pp. 69–85, 2016.

[18] F. Krzalaka, C. Moore, E. Mossel, J. Neeman, A. Sly, and L. Zdeborova, "Spectral redemption in clustering sparse networks," *Proceedings of the National Academy of Sciences of the United States of America*, vol. 110, no. 52, pp. 20 935–20 940, Nov. 2013.

[19] J. Blitzstein and P. Diaconis, "A sequential importance sampling algorithm for generating random graphs with prescribed degrees," *Internet Mathematics*, vol. 6, no. 4, pp. 489–522, 2010.

[20] C. I. del Genio, H. Kim, Z. Toroczkai, and K. E. Bassler, "Efficient and exact sampling of simple graphs with given arbitrary degree sequence," *PLoS ONE*, vol. 5, no. 4, p. e10012 (7 pages), April 2010.